Xia, D.; Chen, X.; Huang, G.; Jiang, B.; Tang, A.; Yanh, H.; Gavras, S.; Huang, Y.; Hort, N.; Pan, F.:
Calculation of Schmid factor in Mg alloys: Influence of stress state.
In: Scripta Materialia. Vol. 171 (2019) 31 - 35.
First published online by Elsevier: 26.06.2019

https://dx.doi.org/10.1016/j.scriptamat.2019.06.014

Calculation of Schmid factor in Mg alloys: Influence of stress state

D. Xia[1,2,3,4] and X. Chen[1,2], G. Huang[1,2,4], B. Jiang[1,2,4], A. Tang[1,2,4], H. Yang[3], S. Gavras[3], Y. Huang[3], N. Hort[3], F. Pan[1,2,4]

[1]State Key Laboratory of Mechanical Transmission, College of Materials Science and Engineering, Chongqing University, Chongqing 400044, China
[2]National Engineering Research Center for Magnesium Alloys, Chongqing University, Chongqing 400044, China
[3]Magnesium Innovation Centre, Helmholtz-Zentrum Geesthacht, Max-Planck-Strasse 1, 21502, Geesthacht, Germany
[4]Chongqing Research Center for Advanced Materials, Chongqing Academy of Science & Technology, Chongqing 401123, China

Abstract

A modified global Schmid factor under different stress states was developed by introducing the stress intensity to normalize the stress tensor. The new method offers an efficient way to compare the activation of one deformation mode under different stress states. The distributions of global Schmid factors for deformation modes in Mg alloys were also studied using this new method. The results indicated that stress state dominated the distributions of global Schmid factors for different deformation modes in a similar way. Additionally, the deformation compatibilities among deformation modes were also influenced by the stress state, especially under a biaxial stress state.

Schmid law states that a slip system can be activated if the resolved shear stress applied to the material is higher than the critical resolved shear stress of this slip system [1]. With the highest Schmid factor (SF), the slip or twinning system has the greatest possibility to be activated [2-4]. Hence, SF is widely used to evaluate the activation of deformation modes, especially for Mg alloys under a uniaxial stress state [5-7]. The resolved shear stress (τ) can be expressed as [8]:

$$\tau = \frac{F\cos\lambda}{(\frac{A}{\cos\varphi})} = \frac{F}{A}\cos\lambda\cos\varphi \tag{1}$$

where F is the loading force applied to the material, A is the section area of the material, λ (ϕ) is the angle between F and the slip (or twinning) direction (normal direction of the plane, ND). The $cos\lambda \cdot cos\phi$ is known as the Schmid factor.

However, Eq. (1) only gives a method to calculate the resolved shear stress or SF under uniaxial stress state, which has a clear load direction.

When the stress state is not uniaxial, such as biaxial or triaxial, it is difficult to calculate the SF using Eq. (1) directly. Hence, methods were developed to solve this problem [9-14]. For instance, during rolling, the SF was taken as the average of SF for tension along the rolling direction (RD) and SF for compression along ND, plus or minus depending on whether the c-axis was extended or compressed [9,10,14]. However, this method could not be used under other stress states. Jin et al. [11] showed the direction of the largest one among three principal stresses was taken as the load direction to calculate SF during three-point bending. The influence of the other two principal stresses on SF was ignored. This method could only be used for qualitative analysis. Chen et al. [15] introduced an effective Schmid factor (ESF) based on the ratio of the external work to the internal work of particular deformation mode. During the calculation of ESF, the Schmid factor was treated as a tensor. Since it is difficult to compare two tensors, ESF was defined as the ratio of resolved shear stress to the effective stress. This ratio could be calculated based on the ratio of the unit external work to the internal work. Recently, a global Schmid factor (GSF) was introduced to describe the activation of deformation modes during rolling or under plane strain state [12,13]. The difference between SF and GSF is that a stress tensor is used as the load on the deformation modes during the calculation of GSF. Set b = (bx, by, bz) as the normalized slip or shearing direction and n = (n_x, n_y, n_z) as normalized ND of the slip or shearing plane. The stress tensor σ is usually simplified as shown by Eq. (2) in the principle stress space where σ_1, σ_2, σ_3 are three principle stresses. Thus, GSF can be calculated as $b^T \cdot \sigma \cdot n$ or specified as Eq. (3):

$$\sigma = \begin{pmatrix} \sigma_x & \tau_{xy} & \tau_{zy} \\ \tau_{xy} & \sigma_y & \tau_{yz} \\ \tau_{zx} & \tau_{yz} & \sigma_z \end{pmatrix} = \begin{pmatrix} \sigma_1 & & \\ & \sigma_2 & \\ & & \sigma_3 \end{pmatrix} \tag{2}$$

$$GSF = b_x\sigma_1 n_x + b_y\sigma_2 n_y + b_z\sigma_3 n_z \tag{3}$$

For slip systems, the final GSF is an absolute value.

The introduction of the stress tensor gives GSF a much broader scope of application under different stress states. However, the GSF is still imperfect. When the stress state is uniaxial, the unique non-zero principle stress can always be simplified as one (e.g. σ_1 = 1 and σ_2 = σ_3 = 0). It infers that for the same deformation mode, the same SF value means the same possibility to be activated, because the loads along different directions are normalized to be "1". In this case, GSF is equivalent to SF with the same range (-0.5- 0.5). However, when the stress state is biaxial or triaxial, there are more than one non-zero principle stresses. According to Eq. (3), the value and the range of GSF will change with different ratios among the non-zero principle stresses. Besides, the stress tensor with one specific ratio (e.g. σ_1 = 1, σ_2 = 1, σ_3 = 0.5) may be not equivalent to another stress tensor with a different ratio (e.g. σ_1 = 0.5, σ_2 = 0.8, σ_3 = 1). It means that for the same deformation modes and the same GSF value may mean that different possibilities could be activated since the loads are not the same scale.

According to von Mises criterion, when the load is over the stress intensity (also known as the equivalent von Mises stress), the material will yield, no matter how diverse the ratios are among the principle stresses [16]. If different stress tensors have the same stress intensity, they are equivalent for the material to yield [17]. Hence, to improve the calculation method of GSF, a stress intensity to normalize the stress tensor is introduced. Eq. (4) and Eq. (5) show the calculation of stress intensity σ using the general stress tensor with shear stress components or simplified stress tensor in the principle stress space. The modified GSF is calculated as Eq. (6).

$$\bar{\sigma} = \sqrt{\frac{(\sigma_x - \sigma_y)^2 + (\sigma_y - \sigma_z)^2 + 6(\tau_{xy}^2 + \tau_{yz}^2 + \tau_{xz}^2)}{2}} \tag{4}$$

$$\bar{\sigma} = \sqrt{\frac{(\sigma_1 - \sigma_2)^2 + (\sigma_2 - \sigma_3)^2 + (\sigma_3 - \sigma_1)}{2}} \tag{5}$$

$$GSF = (b^T \cdot \sigma \cdot n)\sqrt{\sigma} \tag{6}$$

Hence, the modified GSF can be used under any kinds of stress states, even though the shear stress components are non-zero or the simplification of stress tensor is not available. It should be noted that the stress intensity $\bar{\sigma}$ based on the von Mises yield criterion is not the same concept with the "effective stress" introduced in Chen et al. [15]. Here we just use the symbol $\bar{\sigma}$ to be in line with the classical plastic theory. To verify this new method, we investigated the

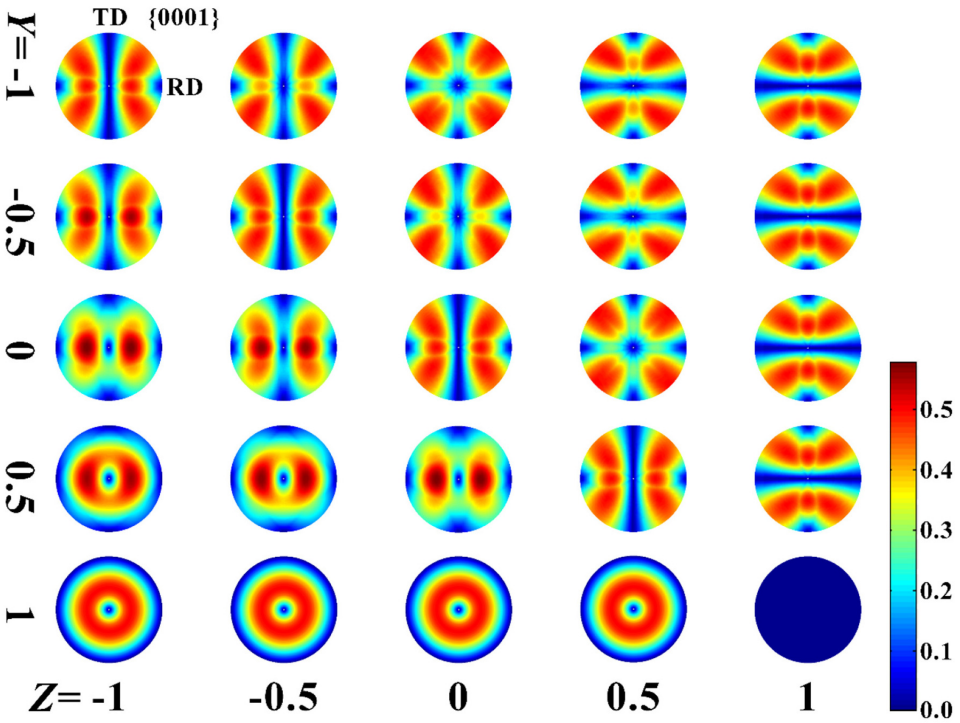

Figure 1: Influence of stress state on the distribution of GSF for basal slip as a function of {0001} PF. The scale is (0-0.58).

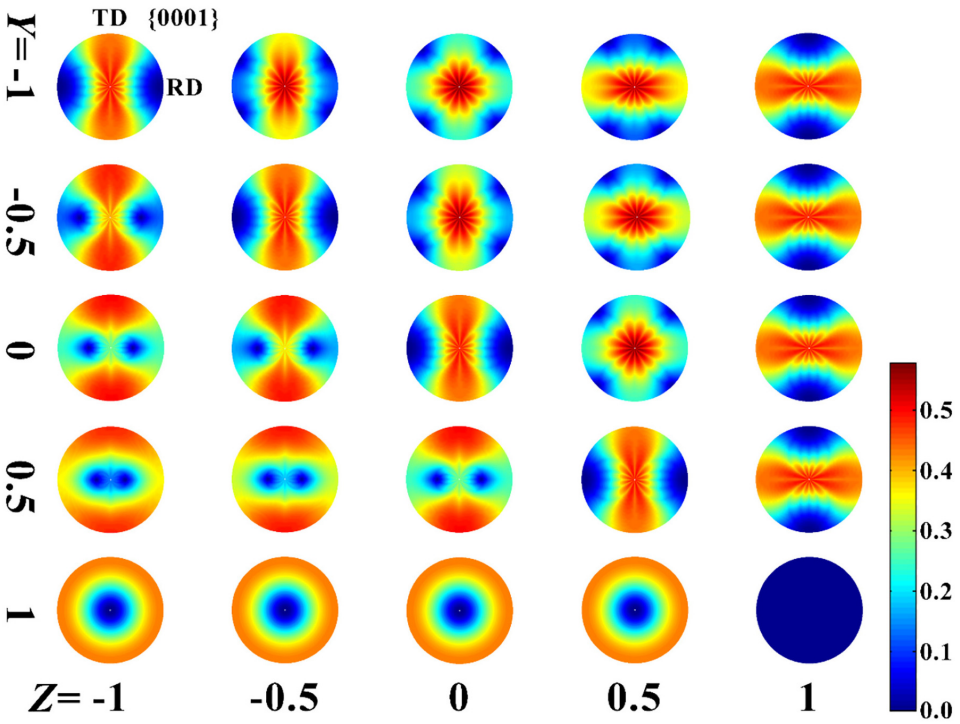

Figure 2: Influence of stress state on the distribution of GSF for prismatic slip as a function of {0001} PF. The scale is (0-0.58).

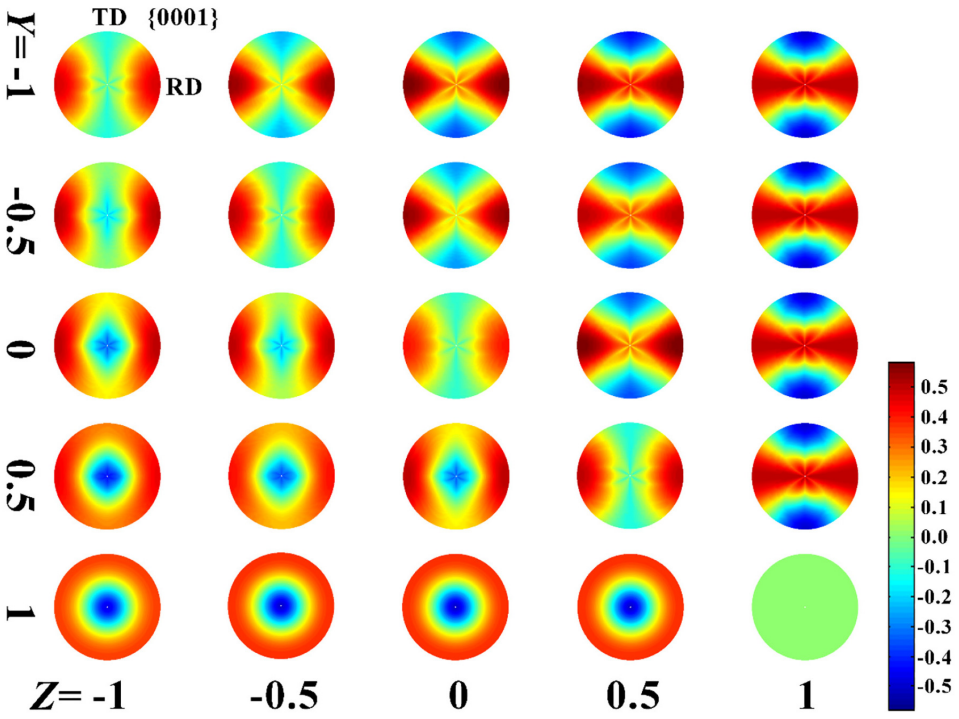

Figure 3: Influence of stress state on the distribution of SF for TT as a function of {0001} PF. The scale is (-0.58-0.58).

Table 1: The ranges of GSFs for basal «a» slip under different stress states. The ratio of X is set as 1.

ZY	-1	-0.5	0	0.5	1
-1	(0-0.50)	(0 - 0.51)	(0-0.50)	(0- 0.51)	(0-0.50)
-0.5	(0-0.55)	(0-0.50)	(0-0.50)	(0-0.50)	(0-0.50)
0	(0-0.58)	(0 - 0.57)	(0-0.50)	(0-0.50)	(0-0.50)
0.5	(0-0.55)	(0 - 0.57)	(0- 0.58)	(0-0.50)	(0-0.50)
1	(0-0.50)	(0-0.50)	(0-0.50)	(0-0.50)	(0-0)

influence of stress states on GSFs for basal «a», prismatic «a» slip systems and tensile twinning (TT) in Mg alloys. During the calculation, we set X-axis, Y-axis and Z-axis along RD, transverse direction (TD) and ND of sample coordination. To simplify the calculations, we set σ_1 = 1 (X = 1) and σ_2 (Y), σ_3 (Z) in a range of (-1-1). Furthermore, the third Euler angle was set to be zero since its influence on the distribution of SF is not significant [18]. The adopted GSF value is the highest value for all the variants of the corresponding mode. The results are shown in Figs. 1-3.

Figs. 1-3 indicate that the stress state dominates the distribution of GSFs for these three deformation modes in a similar way. Firstly, all distribution of GSFs changes gradually from axisymmetric to circularly symmetric with the Y ratio changing from -1 to 1. Besides, the four corners of Figs. 1-3 represent four kinds of distributions of high GSFs in the pole figures (PFs), which are determined by the stress state. Close to upper left or right corner, the distribution of high GSFs tends to be parallel to TD or RD. The lower left corner means a circular symmetric distribution. The GSF distribution at the lower right corner will be discussed later. Hence, according to the distribution of GSFs, Mg alloys with different textural orientations will show different deformability under different stress states [19-21]. The symmetries of the GSF distributions in the inner PFs are a little different according to different modes. The special distributions of GSF at the centers of some PFs are mainly attributed to the sensitivity of trigonometric functions to the change of Euler angles in this region, especially as shown in Fig. 2 or Fig. 3. In addition, the Z ratio affects the values of GSFs but has no influence on the symmetry of the GSF distribution when X: Z = 1:1. A similar phenomenon is found when X:Z = 1:1, but the changing ratio of Y has no influence on the symmetry of GSF distribution as well. This kind of similarity comes from the symmetry of stress states. The distribution of GSFs can be exported under other kinds of stress states based on this stress state symmetry as well.

Secondly, with different stress ratios, the range of GSF will change also. As an example, Table 1 shows the different ranges of GSFs for basal «a» slip under

different stress states. From the results presented, the highest GSF for basal «a» slip is with stress ratios of X: Y:Z = 1:0:-1 or X:Y:Z = 1:0.5:0. However, the ESF value for basal slip reported by Chen et al. can be about 0.8 under the stress state with σ_{12} and w = $\pm$10 [15]. To investigate this difference, the elastic work involved by Chen et al. can be calculated using Eq. (7) in the principle stress space:

$$U_{ex} = \frac{1}{2E}[\sigma_1^2 + \sigma_2^2 + \sigma_3^2 - 2\nu(\sigma_1\sigma_2 + \sigma_2\sigma_3 + \sigma_3\sigma_1)] \tag{7}$$

The elastic work consists of two components: the volumetric work and the distortional work. The volumetric work is calculated as:

$$W_\nu = \frac{1-2\nu}{6E}(\sigma_1 + \sigma_2 + \sigma_3)^2 \tag{8}$$

The distortional work is calculated as:

$$W_d = U_{ex} - W_\nu = \frac{1+\nu}{3E}\bar{\sigma}^2 \tag{9}$$

Here $\bar{\sigma}$ is the stress intensity. Hence, the physical interpretation of von Mises yield criterion offered by Hencky et al. suggested that yielding began when the distortion work reached a critical value [22]. Since Poisson's ratio and the elastic modulus are constants to materials, this interpretation is equivalent to the interpretation based on the stress intensity mentioned above. It means that the difference between ESF and the modified GSF mainly comes from the consideration of the volumetric work and the range change caused by the parameters. Hence, GSF normalized by the stress intensity is a better choice than ESF when the influence of the volumetric work is ignored and vice versa. Additionally, when the stress ratio is X:Y:Z = 1:1:1 (at the lower right corner mentioned above), the GSF for any mode with any orientation is always zero. This means that no deformation modes can be activated under equal tri-axial stress state. The main reason is that the total stress is along ND of the slip or twinning plane under equal triaxial stress state, which leads to no shear stress in the plane. Hence, materials are always brittle under equal triaxial tensile stress state and always ductile under equal tri-axial compressive stress state [23]. There should also be a gradual change of GSF range when the stress state is close to X:Y:Z = 1:1:1. However, since we have normalized the stress tensor by stress intensity, this transition is neutralized. Hence, during processing based on slips or twinning, the appearance of equal or quasi-equal triaxial stress state in Mg alloys should be avoided.

Finally, the special distribution of GSFs also affects the compatibility between slips and TT. For example, a grain in Mg alloys with c-axis parallel to RD can deform by TT, and the c-axis in the TT variant is parallel to ND under a biaxial

tensile stress state [24]. According to Figs. 1-3, the high GSF for prismatic «a» slip will decrease from approximately 0.5 to 0 in the TT variant, which means the appearance of tensile twins will give a limit to the activation of prismatic «a» slip. This kind of incompatibility is easier to happen for Mg alloys under the stress states that can lead to a circular symmetry distributed GSF for deformation modes, such as the biaxial stress state. That is also partially the reason for the lack of easy deformation modes to accommodate plastic strain in Mg alloy rolled sheets with strong basal texture during formation [25-28]. Hence, in order to improve the formability of Mg alloys, the influence of the stress state should also be considered.

In summary, by normalizing the stress tensor and modifying the calculation method, the new GSF can be used to compare the possibilities of the same deformation mode under different stress states. Using this method, the distribution of GSFs for basal, prismatic slip and TT in magnesium alloys was proved to be dominated by the stress state. In addition, all the deformation modes would be limited if the stress state was equal or quasi-equal triaxial. The compatibility between slips and twinning was dominated by stress state as well. Based on these conclusions, Mg alloys with proper orientations can be chosen to obtain different deformability or identify the activation of deformation modes under different stress states.

Acknowledgements

This work was supported by China National Key Research and Development Plan Project (2016YFB0301104), the National Natural Science Foundation of China (No. 51671041, No. 51531002 and No. U1764253) and Natural Science Foundation of Chongqing (cstc2017jcyjBX0040). The China Scholarship Council is also gratefully acknowledged for financial support for Dabiao Xia (201806050045).

References

1. E. Schmid, W. Boas, Hughes & Co. Ltd, 1950 112-117.

2. Y.N. Wang, C.I. Chang, C.J. Lee, H.K. Lin, J.C. Huang, Scripta Mater. 55 (7) (2006) 637-640.

3. A. Javaid, F. Czerwinski, J. Magnes. Alloy 7 (1) (2019) 27-37.

4. L.L.C. Catorceno, H.F.G. de Abreu, A.F. Padilha, J. Magnes. Alloy 6 (2) (2018) 121-133.

5. L.H. Song, B.L. Wu, L. Zhang, X.H. Du, Y.N. Wang, C. Esling, Mat. Sci. Eng. A 710 (2018) 57-65.

6. G.D. Sim, G. Kim, S. Lavenstein, M.H. Hamza, H.D. Fan, J.A. El-Awady, Acta Mater. 144 (2018) 11-20.

7. Z. Zhang, Y.T. Zhang, J.S. Zhang, Y. Li, Y.B. Ma, C.X. Xu, J. Magnes. Alloy 6 (3) (2018) 255-262.

8. J. Pan, J. Tong, M. Tian, Tsinghua, vol. 144, University Press, 2011.

9. J.R. Luo, A. Godfrey, W. Liu, Q. Liu, Acta Mater. 60 (5) (2012) 1986-1998.

10. M.R. Barnett, Z. Keshavarz, M.D. Nave, Metall. Mater. Trans. A 36 (7) (2005) 1697-1704.

11. L. Jin, J. Dong, J. Sun, A.A. Luo, Int. J. Plasticity 72 (2015) 218-232.

12. Y.S. Choi, H.R. Piehler, A.D. Rollett, Metall. Mater. Trans. A 35 (2) (2004) 513-524.

13. C. Guo, Chongqing University, China (Phd. thesis) (2016).

14. I. Dillamore, W. Roberts, Acta Metall. 12 (3) (1964) 281-293.

15. S.-F. Chen, H.-W. Song, S.-H. Zhang, M. Cheng, C. Zheng, M.-G. Lee, Scripta Mater. 167 (2019) 51-55.

16. A. Preumont, V. Piefort, J. Vib. Acoust. 116 (2) (1994) 245-248.

17. R.V, Mises, Mathematisch-Physikalische Klasse (1913) 586-606.

18. O.E.A.V. Randle, Group 2 (2010) 34-36.

19. H.L. Kim, W.K. Bang, Y.W. Chang, Mat. Sci. Eng. A-Struct. 552 (2012) 245-251.

20. T.T.T. Trang, J.H. Zhang, J.H. Kim, A. Zargaran, J.H. Hwang, B.C. Suh, N.J. Kim, Nat. Commun. 9 (2018).

21. A.E. Davis, J.D. Robson, M. Turski, Acta Mater. 158 (2018) 1-12.

22. H. H, Z. Angew. Math. Mech. 4 (4) (1924) 323-334.

23. R.M. Christensen, Oxford University Press (2013) 86.

24. D.B. Xia, G.S. Huang, Q.Y. Deng, B. Jiang, S.S. Liu, F.S. Pan, Mat. Sci. Eng. A 715 (2018) 379-388.

25. S.J. Kim, C. Lee, J. Koo, J. Lee, Y.S. Lee, D. Kim, Mat. Sci. Eng. A 724 (2018) 156-163.

26. M. Jahedi, B.A. McWilliams, P. Moy, M. Knezevic, Acta Mater. 131 (2017) 221-232.

27. Q. Wang, B. Jiang, A. Tang, C. He, D. Zhang, J. Song, T. Yang, G. Huang, F. Pan, Mat. Sci. Eng. A 746 (2019) 259-275.

28. J.H. Zhang, S.J. Liu, R.Z. Wu, L.G. Hou, M.L. Zhang, J. Magnes. Alloy 6 (3) (2018) 277-291.